Journal of
Mechanics of
Materials and Structures

CONSISTENT LOADING FOR THIN PLATES

Isaac Harari, Igor Sokolov and Slava Krylov

Volume 6, No. 5 May 2011

mathematical sciences publishers

JOURNAL OF MECHANICS OF MATERIALS AND STRUCTURES
Vol. 6, No. 5, 2011

msp

CONSISTENT LOADING FOR THIN PLATES

ISAAC HARARI, IGOR SOKOLOV AND SLAVA KRYLOV

Structural models are well-established for the governing operators in solid mechanics, yet the reduction of loads (data) is often performed in an *ad hoc* manner, which may be inadequate for the complex load distributions that often arise in modern applications. In the present work we consistently convert three-dimensional data to the form required by Kirchhoff thin-plate theory, in a variational framework. We provide formulas for all types of resultant structural loads and boundary conditions in terms of the original three-dimensional data, including proper specification of corner forces, in forms that are readily incorporated into computational tools. In particular, we find that in-plane components of three-dimensional loads engender distributed couples, contributing to an effective distributed transverse force and boundary shear force, the latter generalizing the notion of the celebrated Kirchhoff equivalent force. However, in virtual work we advocate a representation of the twisting moment in a form that involves neither the Kirchhoff equivalent force nor corner forces. An interpretation of the structural deflections as through-the-thickness averages of the continuum displacements, rather than their values on the midplane, yields explicit formulas for the thin-plate essential boundary data. The formulation facilitates the solution of problems that would otherwise pose formidable challenges. Numerical results confirm that appropriate use of the thin-plate model economizes computation and provides insight into the mechanical behavior, while preserving a level of accuracy comparable with the full three-dimensional solution.

1. Introduction

In solid mechanics the common approach to the analysis of bodies with distinctive geometric characteristics is to perform a dimensional reduction to an appropriate structural model. The analytical solution for these bodies is difficult for general geometries and loadings while the computation is often costly. A classical example is a plate-like body which is commonly described by a thin-plate model.[1] The dimensional reduction of the differential operator describing the original elasticity problem is often performed by variational procedures combined with certain kinematic and constitutive assumptions [Alessandrini et al. 1999; Hu 1984; Soedel 1981; Vidoli and Batra 2000]. This technique can be considered as a restriction of an approach applied to shells [DiCarlo et al. 2001]. Alternatively, hierarchies of reduced-order models of elastic bodies with high aspect ratio are built using asymptotic methods [Ciarlet 1990; Dauge and Gruais 1996; Dauge and Gruais 1998].

Since the thin-plate theory (Kirchhoff theory) has been developed [Kirchhoff 1850; Poisson 1829] based on fundamental contributions by Siméon-Denis Poisson (1811) and Gustav Robert Kirchhoff (1850) (see also [Timoshenko 1983; Todhunter and Pearson 1960] for historical treatises) a large variety

Keywords: Kirchhoff thin-plate theory, structural reduction, Kirchhoff equivalent force, distributed couples, corner forces.

[1] We distinguish between a *plate*, which is a flat structure that has thickness much smaller than the other dimensions, and a *plate model* or *theory*, which is the collection of assumptions that is used to dimensionally reduce the three-dimensional formulation and approximate its solution.

of models were built starting from simple plates theories [Reissner 1969; Sayir and Mitropoulos 1980] and up to nonlinear [Antman 1995; Ciarlet 1997; Libai and Simmonds 1998; Rubin 2000] and composite [Bisegna and Sacco 1997; Calcote 1969; Vasil'ev and Lur'e 1992] plates and shells. Extensive research was performed also in connection with numerical methods [Actis et al. 1999; Engel et al. 2002; Hughes and Hinton 1986; O'Leary and Harari 1985; Vogelius and Babuška 1981]. See also the reviews [Podio-Guidugli 2000; Sayir and Mitropoulos 1980].

In the construction of different structural theories, the procedures of reduction of elastic continua by the appropriate structural models are conventionally based on the body geometry determining the order of the small parameter used in the reduction. However, while such procedures are well-established for the differential operators governing problems of solid mechanics in general and plate-like problems in particular, the reduction of the data of the problem — body forces and boundary conditions — is often performed in an *ad hoc* manner. The form of the loading for problems that are governed by reduced structural theories is quite different from that of the original three-dimensional formulation. As a result, the *ad hoc* approach based on engineering intuition can be inadequate for the analysis of bodies subject to complex three-dimensional loading, and more rigorous procedures are required.

As an example of problems where complex three-dimensional loading is abundant one can mention coupled problems distinguished by the distribution of loading arising as a result of interaction. In the intrinsically multiphysics problems arising in micro and nanoelectromechanical systems (MEMS and NEMS) based applications the interaction forces are obtained in terms of electric or magnetic fields. The distribution of electrostatic or magnetic forces could produce very complex three-dimensional patterns which may include, for example, distributed couples (see [Liu and Chang 2005; Moon and Holmes 1979] and references therein). High aspect ratios of microstructures incorporated in MEMS make the use of structural descriptions attractive. However, due to intricate character of the three-dimensional interface forces, *ad hoc* procedures for their reduction are no longer sufficient. Other applications where the structural representation could be effective but *ad hoc* formulation of the reduced loading is not sufficient include aeroelastic and hydroelastic applications where the loading conditions are formulated in terms of interface velocities or contact pressures [Morand and Ohayon 1995]. High aspect ratios of aero/hydroelastic structures make the use of computationally efficient models based on the structural descriptions attractive, especially when incorporated in optimization or control procedures. For example, entire airplane wings or helicopter blades are routinely modeled as one-dimensional (beams) and two-dimensional structural elements (plates) of variable cross-section. On the other hand, the high gradients and intricacy of interface forces arising in these applications may require three-dimensional representation of the data. One can also mention problems involving complex spatially distributed surface forces originating in contact. This kind of force arises, for example, during forming processes of thin (i.e., high aspect ratio) metal sheet. In these processes surface tractions distributed in the direction tangent to the surface originate mainly from friction between the surfaces of the forming tool and the metal sheet.

The implementation of rigorous reduction procedures which use a variational framework and allow systematic reduction of the three-dimensional loading data to their structural counterparts for beam-like solids was analyzed in [Krylov et al. 2006]. In this work, we extend the implementation of these reduction procedures to the thin (Kirchhoff-Love) plate model. Despite its limitations, Kirchhoff-Love theory of thin-plate bending is one of the most widely used by engineers, mainly due to its simplicity. Nowadays, descriptions of thin bending theory can be found in most textbooks on structural mechanics (e.g., see

[Nádai 1925; Sokolnikoff 1983; Timoshenko and Goodier 1951; Timoshenko and Woinowsky-Krieger 1959; Ugural 1981]).

In the present work special attention is paid to the rigorous reduction, by means of a variational procedure, of the original problem data to the form required by the structural representation. The structural counterparts of the loads are expressed in terms of the data of the original three-dimensional problem. Note that in most cases, in considering bending of plates in the framework of the classical thin-plate theory only transverse loads, namely, loads acting in the direction perpendicular to the plate's plane in a three-dimensional domain, are accounted for. We show that consistent consideration of three-dimensional applied in-plane body forces and surface tractions in the classical thin-plate formulation engenders distributed couples, modifying the Kirchhoff equivalent shear force and the transverse distributed force [DiCarlo et al. 2001; Niordson 1985]. In addition, we present a consistent treatment of essential (kinematic) boundary conditions. Structural counterparts of the essential boundary conditions considered here as through-the-thickness averages [Cowper 1966; Prescott 1942] are obtained in terms of three-dimensional displacements (which generally speaking would not conform the structural assumptions) prescribed on an appropriate part of the surface. It should be noted that certain aspects of thin-plate theory, for example, corner forces arising at the points of discontinuity of the plate's outer boundary, are treated differently in the literature by various sources. Using the systematic variational approach, we confirm that corner forces are actually a part of the natural boundary conditions.

The goal of the work is twofold. First, the results of the work provide better insight into the contribution of different components of data into the structural model. In addition, the structural form of the weak formulation derived systematically from the original three-dimensional elasticity expressions along with essential boundary conditions expressed in terms of the original three-dimensional data are useful as a basis for numerical procedures.

In Section 2 the differential equations and the natural boundary conditions for plate-like bodies are derived from the variational principle. We begin with the formulation of the three-dimensional elastic problem, substitute the kinematic and constitutive assumptions into the variational equation and derive the classical Kirchhoff-Love thin-plate equations and boundary conditions. The validation of the models is performed in Section 3 by comparison to analytical solutions of torsionless axisymmetric elasticity problems. The estimation of the structural efficiency from the computational point of view is performed in Section 4, by comparison to a three-dimensional elasticity problem solved by the finite element method.

2. Structural reduction of elastostatics by the thin-plate model

The dimensional reduction of the elasticity operator in thin flat bodies by various plate models, as outlined above, is a well-established procedure. The reduced structural models are expressed in terms of unknown deflections. When these deflections are found, recovery procedures are available to approximate the three-dimensional displacement field.

The goal of the present work is to derive a systematic conversion of general three-dimensional loads to their structural counterparts, in forms that are readily incorporated into computational tools.

2A. ***Assumptions of Kirchhoff plate theory.*** The domain is a three-dimensional thin flat body (Figure 1) defined by

$$\Omega = \{(x_1, x_2, x_3) \in \mathbb{R}^3 \mid (x_1, x_2) \in A,\ -t/2 < x_3 < t/2\}. \tag{2-1}$$

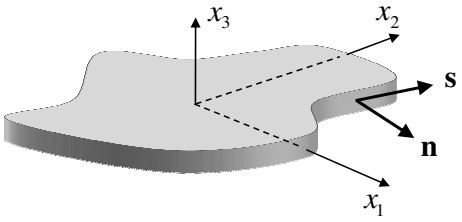

Figure 1. Geometry of a thin flat body.

Here t is the plate thickness, which may vary with x_1 and x_2, and $A \subset \mathbb{R}^2$ is the midplane of the plate.

The kinematic assumptions of the classical Kirchhoff plate theory approximate the displacements u_i by structural counterparts

$$u^s_\alpha(x_1, x_2, x_3) = w_\alpha(x_1, x_2) - x_3 w_{3,\alpha}(x_1, x_2), \tag{2-2}$$

$$u^s_3(x_1, x_2, x_3) = w_3(x_1, x_2). \tag{2-3}$$

The structural displacements are defined in terms of in-plane (stretching) w_α and transverse (bending) w_3 deflections. In the following, the deflections are considered as through-the-thickness averages (although commonly associated with the midplane). Throughout, Latin indices i, j, k, l take on values 1, 2, 3, Greek indices $\alpha, \beta, \gamma, \delta$ take on values 1, 2. The summation convention over repeated indices is applied. In addition, $(\cdot)_{,\alpha} = \partial(\cdot)/\partial x_\alpha$ is used for the partial derivative. From expressions (2-2) and (2-3) the approximate three-dimensional displacements u^s_i can be recovered after determining w_i.

Strains in the x_3-direction are not computed from the displacements but via the constitutive assumption of plane stress

$$\sigma^s_{33} = 0. \tag{2-4}$$

In the homogeneous isotropic case, considered here for simplicity, the strains are

$$\epsilon^s_{\alpha\beta} = u^s_{(\alpha,\beta)} = w_{(\alpha,\beta)} - x_3 w_{3,\alpha\beta}, \qquad \epsilon^s_{\alpha 3} = u^s_{(\alpha,3)} = 0, \qquad \epsilon^s_{33} = \frac{-\nu}{1-\nu}\epsilon^s_{\alpha\alpha}. \tag{2-5}$$

Here, $w_{(\alpha,\beta)}$ are the in-plane strains and $w_{3,\alpha\beta}$ are the curvatures. Parentheses in the subscripts denote the symmetric part of a tensor: $t_{(\alpha\beta)} = \frac{1}{2}(t_{\alpha\beta} + t_{\beta\alpha})$. The resulting two-dimensional constitutive relations are

$$\sigma^s_{\alpha\beta} = \frac{E}{1+\nu}\left(\frac{\nu}{1-\nu}\delta_{\alpha\beta}\epsilon^s_{\gamma\gamma} + \epsilon^s_{\alpha\beta}\right). \tag{2-6}$$

Here, E and ν are Young's modulus and Poisson's ratio respectively. Following convention in Kirchhoff plate theory, $\sigma^s_{\alpha 3}$ are evaluated from equilibrium rather than from the constitutive relations.

The structural reduction is performed in a variational framework, following the description in [Hughes 2000]. Special attention is paid to the reduction of distributed boundary data and body forces to their structural equivalents.

2B. ***Virtual work.*** Consider the standard linear elastostatics boundary-value problem in the bounded domain $\Omega \subset \mathbb{R}^3$, with boundary Γ. The boundary of the domain consists of the top and bottom surfaces ($x_3 = \pm t/2$) and the lateral boundary, assumed to be a cylindrical surface. The boundary Γ has subregions

Γ_g and Γ_h such that $\Gamma = \Gamma_g \cup \Gamma_h$ and $\Gamma_g \cap \Gamma_h = \varnothing$. The data (loads) are prescribed displacements $g_i : \Gamma_g \to \mathbb{R}$ (essential boundary conditions), tractions $h_i : \Gamma_h \to \mathbb{R}$ (natural boundary conditions) and body forces $f_i : \Omega \to \mathbb{R}$. In general, the boundary may admit different decompositions for different components. The procedure is formulated in terms of Γ_g and Γ_h for simplicity of presentation. Extensions to more general cases are straightforward and considered subsequently.

The plate equations, including expressions for structural loads expressed in terms of the original three-dimensional data, are obtained from the standard variational formulation for the elasticity theory. This is the principle of virtual work: find u_i that satisfies $u_i = g_i$ on Γ_g such that

$$\int_\Omega \bar{u}_{(i,j)}\sigma_{ij}\, d\Omega = \int_\Omega \bar{u}_i f_i\, d\Omega + \int_{\Gamma_h} \bar{u}_i h_i\, d\Gamma. \tag{2-7}$$

Here, $\bar{u}_i$ is the weighting function, or variation, satisfying the homogenous counterpart of the essential boundary conditions $\bar{u}_i = 0$ on Γ_g. The stress σ_{ij} is defined in terms of the displacement u_i via strain in the usual way.

To fix ideas, consider applied displacements and tractions on corresponding parts of the lateral boundary, whereas only tractions are specified on the top and bottom surfaces ($x_3 = \pm t/2$). (This configuration is common in practice.) The lateral boundary has a unit outward normal vector $\boldsymbol{n} = n_\alpha \boldsymbol{e}_\alpha$ and a unit tangent vector $\boldsymbol{s} = s_\alpha \boldsymbol{e}_\alpha$, such that $\boldsymbol{n} \times \boldsymbol{s} = \boldsymbol{e}_3$ (Figure 1). Here, the $\boldsymbol{e}_i$ are the Euclidean basis unit vectors. On part of the lateral boundary (Γ_g) we consider essential boundary conditions specified by the transverse displacement g_3 and the normal and tangential in-plane displacements $g_n = g_\alpha n_\alpha$ and $g_s = g_\alpha s_\alpha$. On the remaining part of the lateral boundary we consider natural boundary conditions specified by the transverse traction h_3 and the normal and tangential in-plane tractions $h_n = h_\alpha n_\alpha$ and $h_s = h_\alpha s_\alpha$.

The boundary of the midplane A, denoted S, is subdivided into two non-overlapping regions S_g (such that $S_g \times [-t/2,\ t/2] = \Gamma_g$) and $S_h = S \setminus S_g$. If S is not smooth, the corners, where the normal vector $\boldsymbol{n}$ suffers a discontinuity, are denoted $\partial S = \{\boldsymbol{x}_c\}_{c=1}^{n_{\text{corn}}}$, where $\boldsymbol{x}_c \in S$ is a corner location and n_{corn} is the number of corners.

The boundary Γ_h is partitioned in such a way that

$$\int_{\Gamma_h} \ldots d\Gamma = \int_A \langle \ldots \rangle\, dA + \int_{S_h} \int_{-t/2}^{t/2} \ldots dx_3\, dS. \tag{2-8}$$

Here, dS is the arc length along S, and the $\langle \ldots \rangle$ operator is defined by

$$\langle f(x_1, x_2, x_3) \rangle = f(x_1, x_2, -t/2) + f(x_1, x_2, t/2).$$

Replacing the displacements u_i and stresses σ_{ij} in (2-7) by their structural counterparts u_i^s and $\sigma_{\alpha\beta}^s$ (since $\sigma_{33}^s = 0$ by the constitutive assumption (2-4) and $u_{(\alpha,3)}^s = 0$ by the kinematic assumptions (2-2) and (2-3)) yields

$$\int_\Omega \bar{u}_{(\alpha,\beta)}^s \sigma_{\alpha\beta}^s\, d\Omega = \int_\Omega (\bar{u}_\alpha^s f_\alpha + \bar{u}_3^s f_3)\, d\Omega + \int_A (\langle \bar{u}_\alpha^s h_\alpha \rangle + \langle \bar{u}_3^s h_3 \rangle)\, dA + \int_{S_h} \int_{-t/2}^{t/2} (\bar{u}_n^s h_n + \bar{u}_s^s h_s + \bar{u}_3^s h_3)\, dx_3 dS. \tag{2-9}$$

Here, $\bar{u}_i^s$ are variations of the structural displacements. The explicit dependence of the structural quantities on x_3 (from the kinematic assumptions) simplifies the domain integration

$$\int_\Omega \ldots d\Omega = \int_A \int_{-t/2}^{t/2} \ldots dx_3\, dA. \tag{2-10}$$

This leads to the principle of virtual work for the thin plate. Data for the plate essential boundary conditions, prescribed boundary deflections W_i and rotation Θ defined in Table 1, are obtained by the procedure outlined in Section 2C. The statement of thin-plate virtual work is: find w_i that satisfies $w_i = W_i$ and $w_{3,n} = \Theta$ on S_g such that

$$\int_A (\overline{w}_{\alpha,\beta} n_{\alpha\beta} - \overline{w}_{3,\alpha\beta} m_{\alpha\beta})\, dA = \int_A (\overline{w}_\alpha F_\alpha - \overline{w}_{3,\alpha} C_\alpha + \overline{w}_3 F_3)\, dA + \int_{S_h} (\overline{w}_n N_n + \overline{w}_s N_s - \overline{w}_{3,n} M_n - \overline{w}_{3,s} M_s + \overline{w}_3 Q)\, dS. \tag{2-11}$$

Here, $\overline{w}_i$ is the weighting function, or variation, satisfying the homogenous counterpart of the thin-plate essential boundary conditions $\overline{w}_i = 0$ and $\overline{w}_{3,n} = 0$ on S_g.

The applied structural loads, distributed forces and couples F_i and C_α, along with boundary forces and moments N_n, N_s, Q, M_n and M_s, defined in terms of the underlying three-dimensional data in Table 1, result from integration through the thickness. The thin-plate constitutive relations are obtained by substituting the relations (2-5) and (2-6) into the definitions for the in-plane force tensor $n_{\alpha\beta}$ and the bending moment tensor $m_{\alpha\beta}$ (Table 1). For constant plate thickness we have

$$n_{\alpha\beta} = \frac{Et}{1+\nu}\left(\frac{\nu}{1-\nu}\delta_{\alpha\beta} w_{\gamma,\gamma} + w_{(\alpha,\beta)}\right), \tag{2-12}$$

$$m_{\alpha\beta} = -D\big[\nu\delta_{\alpha\beta} w_{3,\gamma\gamma} + (1-\nu) w_{3,\alpha\beta}\big]. \tag{2-13}$$

Here, $D = \dfrac{Et^3}{12(1-\nu^2)}$ is the isotropic bending stiffness.

Remarks. (1) The principle of virtual work for thin plates, (2-11), incorporates applied distributed couples C_α, engendered by in-plane components of three-dimensional loads. This is rarely done in the context of a Kirchhoff plate model. There are three-dimensional load configurations for which distributed couples constitute a significant portion of the resultant structural load. In such cases, omitting these terms in the structural model will disregard a substantial part of the response.

(2) The virtual work equation (2-11) represents two uncoupled two-dimensional problems, an in-plane problem weighted by $\overline{w}_\alpha$ and a plate bending problem weighted by $\overline{w}_3$.

(3) Assuming sufficient regularity of the prescribed boundary twisting moment M_s along smooth parts of S_h, the term representing the external work it exerts within the virtual work equation (2-11) may be integrated by parts, yielding for the bending terms

$$\int_{S_h} (-\overline{w}_{3,n} M_n - \overline{w}_{3,s} M_s + \overline{w}_3 Q)\, dS = \int_{S_h} \big(-\overline{w}_{3,n} M_n + \overline{w}_3 (M_{s,s} + Q)\big)\, dS - (\overline{w}_3 [\![M_s]\!])|_{\partial S \cap S_h}. \tag{2-14}$$

Here, $[\![M_s]\!] = \lim_{\varepsilon\to 0} M_s(\boldsymbol{x}_c + \varepsilon \boldsymbol{s}) - M_s(\boldsymbol{x}_c - \varepsilon \boldsymbol{s})$ represents a corner force. On the right-hand side of (2-14) are the conventional terms that appear regularly as part of the thin-plate virtual work

Quantity	Description
$n_{\alpha\beta} = \int_{-t/2}^{t/2} \sigma^s_{\alpha\beta} dx_3$	in-plane force tensor
$m_{\alpha\beta} = \int_{-t/2}^{t/2} \sigma^s_{\alpha\beta} x_3\, dx_3$	bending moment tensor
$F_\alpha = \int_{-t/2}^{t/2} f_\alpha\, dx_3 + \langle h_\alpha \rangle$	applied in-plane force
$\hat{F}_3 = F_3 + C_{\alpha,\alpha}$	effective applied transverse force
$F_3 = \int_{-t/2}^{t/2} f_3\, dx_3 + \langle h_3 \rangle$	applied transverse force
$C_\alpha = \int_{-t/2}^{t/2} f_\alpha x_3\, dx_3 + \langle h_\alpha x_3 \rangle$	applied couple
$W_n = \frac{1}{t} \int_{-t/2}^{t/2} g_n\, dx_3$	prescribed normal boundary deflection
$W_s = \frac{1}{t} \int_{-t/2}^{t/2} g_s\, dx_3$	prescribed tangential boundary deflection
$W_3 = \frac{1}{t} \int_{-t/2}^{t/2} g_3\, dx_3$	prescribed transverse boundary deflection
$\Theta = -\frac{12}{t^3} \int_{-t/2}^{t/2} g_n x_3\, dx_3$	prescribed tangential boundary rotation
$N_n = \int_{-t/2}^{t/2} h_n\, dx_3$	prescribed normal boundary in-plane force
$N_s = \int_{-t/2}^{t/2} h_s\, dx_3$	prescribed tangential boundary in-plane force
$M_n = \int_{-t/2}^{t/2} h_n x_3\, dx_3$	prescribed boundary bending moment
$\hat{Q} = Q + M_{s,s} - C_n^-$	effective prescribed boundary shear force
$Q = \int_{-t/2}^{t/2} h_3\, dx_3$	prescribed boundary shear force
$M_s = \int_{-t/2}^{t/2} h_s x_3\, dx_3$	prescribed boundary twisting moment
$C_n^-(\boldsymbol{x}) = \lim_{\boldsymbol{\xi} \to \boldsymbol{x}} C_n(\boldsymbol{\xi}),\ \boldsymbol{x} \in S_h$	the edge trace of applied couple
$R = [\![M_s]\!]$	prescribed boundary shear force at corner $\boldsymbol{x}_c$

Table 1. Structural nomenclature. We have set $[\![M_s]\!] = M_s(\boldsymbol{x}_c^+) - M_s(\boldsymbol{x}_c^-)$, where $M_s(\boldsymbol{x}_c^\pm) = \lim_{\varepsilon \to 0} M_s(\boldsymbol{x}_c \pm \varepsilon \boldsymbol{s})$; $f_n = f_\alpha n_\alpha$, $f_s = f_\alpha s_\alpha$; and $\boldsymbol{x}_c \in S$, for $c = 1, 2, \ldots, n_{\text{corn}}$, is a corner location.

equation in the literature [Bauchau and Craig 2009; Šolín 2006], though both forms are mentioned in [Zienkiewicz and Taylor 2000]. The right-hand side indicates the source of the Kirchhoff equivalent (modified shear) force and the corner forces. Indeed, this form appears in the Euler–Lagrange equations (2-15) below and is essential for the strong form of the boundary-value problem. However, the two forms are equivalent statements of virtual work, subject to the higher regularity requirement on the prescribed boundary twisting moment. We prefer the formulation (2-11) as it is simpler and less constrained, compatible with the variational statement of higher-order plate theories, and obviates the use of the Kirchhoff equivalent force and corner forces (thereby allowing lower regularity of the data and facilitating implementation) in methods based on virtual work such as finite element analysis.

(4) All of the loading terms on the right-hand side of the virtual work equation (2-11) may be incorporated by users into commercial finite element computations without re-programming of the software by using the usual definitions of consistent nodal loads.

Integration by parts yields the Euler–Lagrange equations for the thin plate:

$$\begin{aligned}0=&\int_A \overline{w}_\alpha(-n_{\alpha\beta,\beta}-F_\alpha)dA+\int_A \overline{w}_3(-m_{\alpha\beta,\alpha\beta}-F_3-C_{\alpha,\alpha})dA+\int_{S_h}\overline{w}_n(n_{nn}-N_n)dS+\int_{S_h}\overline{w}_s(n_{ns}-N_s)dS\\&+\int_{S_h}\overline{w}_3(m_{\alpha\beta,\beta}n_\alpha+(m_{ns})_{,s}+C_n^-Q-M_{s,s})dS+(\overline{w}_3[\![-m_{ns}+M_s]\!])|_{\partial S\cap S_h}\\&+\int_{S_h}\overline{w}_{3,n}(-m_{nn}+M_n)dS.\end{aligned}\tag{2-15}$$

Here, $(\cdot)_{nn}=(\cdot)_{\alpha\beta}n_\alpha n_\beta$ and $(\cdot)_{ns}=(\cdot)_{\alpha\beta}n_\alpha s_\beta$ denote the normal and tangential components of the stress resultants. Similarly, $(\cdot)_{,n}=(\cdot)_{,\alpha}n_\alpha$ and $(\cdot)_{,s}=(\cdot)_{,\alpha}s_\alpha$ are used for normal and tangential derivatives, respectively.

The three-dimensional boundary value problem of linear elasticity is reduced to a set of two uncoupled two-dimensional boundary-value problems: an in-plane problem and a plate bending problem. Thin plate equilibrium equations are obtained from the area integrals of (2-15) and the thin-plate natural boundary conditions are obtained from the line integrals of (2-15), along with the discrete corner conditions.

2C. ***Essential boundary conditions.*** Structural essential boundary conditions are imposed on the quantities associated with a variation in the boundary integrals of (2-15). The data are specified by a through-the-thickness averaging procedure [Cowper 1966; Prescott 1942] suggested by the definition of the force resultants. The kinematic assumptions (2-2) and (2-3) yield

$$w_i(x_1,x_2)=\frac{1}{t}\int_{-t/2}^{t/2}u_i^s(x_1,x_2,x_3)\,dx_3,\tag{2-16}$$

$$w_{3,n}(x_1,x_2)=-\frac{12}{t^3}\int_{-t/2}^{t/2}u_n^s(x_1,x_2,x_3)x_3\,dx_3.\tag{2-17}$$

Averaging the prescribed three-dimensional displacements on Γ_g yields the thin-plate essential boundary conditions

$$w_i=W_i,\qquad w_{3,n}=\Theta\qquad\text{on } S_g,\tag{2-18}$$

in terms of the prescribed boundary deflections W_i and rotation Θ (Table 1).

Remark. The common view of deflections as displacements of the midplane

$$w_i(x_1,x_2)=u_i^s(x_1,x_2,0)\tag{2-19}$$

may also be used to specify the plate essential boundary conditions (except for the boundary rotation). If the prescribed displacements g_i conform to the kinematic assumptions, the two approaches are equivalent for the boundary deflections. In general, we prefer to interpret deflections as displacements averaged through the thickness.

2D. ***Strong form of Kirchhoff plate problems.*** As noted, the three-dimensional linear elasticity boundary value problem is reduced to two uncoupled two-dimensional problems:

(1) An in-plane problem for $w_\alpha(x_1, x_2)$;

(2) A plate bending problem for $w_3(x_1, x_2)$.

The differential equations and natural boundary conditions are Euler–Lagrange equations emanating from (2-15). Essential boundary conditions are obtained by the through-the-thickness averaging procedure.

The features of the in-plane problem are conventional, and included here for completeness. The in-plane boundary-value problem is

$$\begin{aligned} -n_{\alpha\beta,\beta} &= F_\alpha \quad \text{in } A, \\ w_n = W_n, \qquad w_s &= W_s \quad \text{on } S_g, \\ n_{nn} = N_n, \qquad n_{ns} &= N_s \quad \text{on } S_h. \end{aligned} \tag{2-20}$$

The structural data are expressed in terms of the original three-dimensional data (Table 1). Boundary conditions are designated in terms that refer to the homogeneous case. For example, a "fixed" boundary condition means that all kinematic quantities are specified (but not necessarily zero). In these terms, (2-20) represents a body fixed on one portion of the boundary and free on the rest. Other possible combinations of normal and tangential boundary conditions are shown in Table 2.

Our formulation of the plate bending problem contains several noteworthy features. The plate bending boundary-value problem is

$$\begin{aligned} -m_{\alpha\beta,\alpha\beta} &= \hat{F}_3 \quad \text{in } A, \\ w_3 = W_3 \qquad w_{3,n} &= \Theta \quad \text{on } S_g, \\ m_{nn} = M_n, \qquad m_{\alpha\beta,\beta} n_\alpha + (m_{ns})_{,s} &= \hat{Q} \quad \text{on } S_h, \\ [\![m_{ns}]\!] &= R \quad \text{on } \partial S \cap S_h. \end{aligned} \tag{2-21}$$

For constant plate thickness, the equilibrium equation reduces to the well-known equilibrium equation of Kirchhoff-Love plate theory in terms of the transverse deflection

$$D\nabla^4 w_3 = \hat{F}_3 \quad \text{in } A. \tag{2-22}$$

Again, the structural data are expressed in terms of the original three-dimensional data (Table 1). The

fixed (*or* clamped)	$w_n = W_n$	$w_s = W_s$
free	$n_{nn} = N_n$	$n_{ns} = N_s$
symmetric	$w_n = W_n$	$n_{ns} = N_s$
skew symmetric	$w_s = W_s$	$n_{nn} = N_n$

Table 2. In-plane problem: common boundary conditions. The designations refer to homogeneous boundary conditions.

distributed loading on the plate is an *effective* transverse force

$$\hat{F}_3 = F_3 + C_{\alpha,\alpha}. \tag{2-23}$$

The standard term is modified by the in-plane divergence of applied couples C_α, engendered by in-plane components of three-dimensional body forces and tangential tractions on the top and bottom surfaces.

Similarly, the shear load is an *effective* boundary shear force

$$\hat{Q} = Q + M_{s,s} - C_n^-. \tag{2-24}$$

The celebrated Kirchhoff equivalent force $Q + M_{s,s}$ [Kirchhoff 1850] is modified by the edge trace of applied couples. It would be difficult to derive these terms intuitively. Such terms are rarely accounted for in the literature [Niordson 1985], and presented in an ad hoc basis [Madureira 2004; Sutyrin and Hodges 1996]. Their origins from in-plane components of three-dimensional loads have not been reported in the literature, to our knowledge. When the boundary is not smooth, shear boundary conditions include discrete corner forces R defined in terms of the prescribed boundary twisting moment, emanating from tangential tractions applied on the lateral boundary (Table 1).

Remarks. (1) The treatment of corner forces in the literature is not uniform. In many instances they are defined as boundary conditions accompanying shear boundary conditions at discrete points, part of the problem statement, as described in (2-21) [Bauchau and Craig 2009; Wells and Nguyen 2007; Grossi and Lebedev 2001; Nayfeh and Pai 2004; Reismann 1988; Tsiatas 2009]. However, corner forces also appear only as reaction forces that are part of the solution [Szilard 2004]. In some descriptions there is no mention of corner forces whatsoever. As outlined above, consistent variational derivation of the plate problem formulation gives rise to the corner forces in the Euler–Lagrange equations, and therefore they should appear explicitly as natural boundary conditions in the problem statement.

(2) Both corner forces and the Kirchhoff equivalent force can be derived from a constrained continuum of grade two material [Forte and Vianello 1988].

In terms that refer to homogeneous boundary conditions, (2-21) represents a body fixed on one portion of the boundary and free on the rest. In general, there should be two boundary conditions at each point: either transverse deflection or shear force, and either tangential rotation or bending moment (Table 3).

Possible combinations of three-dimensional data specified at a lateral boundary point with the corresponding type of structural boundary conditions are listed in Table 4. Due to the presence of the Kirchhoff

fixed (*or* clamped)	$w_3 = W_3$	$w_{3,n} = \Theta$	
free	$m_{nn} = M_n$	$(m_{n\alpha})_{,\alpha} + (m_{ns})_{,s} = \hat{Q}$	$[\![m_{ns}]\!] = R$
simply supported	$w_3 = W_3$	$m_{nn} = M_n$	
symmetric	$w_{3,n} = \Theta$	$(m_{n\alpha})_{,\alpha} + (m_{ns})_{,s} = \hat{Q}$	$[\![m_{ns}]\!] = R$

Table 3. Plate bending problem: common boundary conditions. The designations refer to homogeneous boundary conditions ("simply supported" = "skew symmetric").

Three-dimensional	In-plane	Bending
$g_n\ g_s\ g_3$	Fixed	Fixed
$g_n\ g_s\ h_3$	Fixed	—
$g_n\ h_s\ g_3$	Symmetric	Fixed
$h_n\ g_s\ g_3$	Skew symmetric	Simply supported
$g_n\ h_s\ h_3$	Symmetric	Symmetric
$h_n\ g_s\ h_3$	Skew symmetric	—
$h_n\ h_s\ g_3$	Free	Simply supported
$h_n\ h_s\ h_3$	Free	Free

Table 4. Possible combinations of data on the lateral boundary. The designations refer to homogeneous boundary conditions.

equivalent force in thin-plate bending, tangential tractions h_s must always accompany transverse tractions h_3 on the lateral boundary. The thin-plate flexure does not distinguish between the specification of tangential displacements g_s and tractions h_s along with transverse displacements g_3 on the lateral boundary (for fixed and simply supported boundary conditions).

3. Analytical model validation

The use of structural theories for analysis of bodies subject to intricate loading brings up questions about the validity of reduced models. The validity of different plate theories is usually justified by geometric considerations in terms of relative thickness. Nevertheless the validity of a plate model is affected also by the loading conditions. In this context, we reiterate the importance of the rigorous reduction procedure of the loads on one hand and the importance of the model validity examination on the other hand.

In the following sections we demonstrate the implementation of the structural reduction procedure using examples of torsionless axisymmetric elasticity problems with analytical solutions. In order to focus on the more interesting bending problem, we consider such loading for the elastic body that results in structural, thin-plate, load resultants for which the in-plane problem has a trivial solution. Validation of reduced structural solutions is performed through comparison with the solutions of the elasticity problem. Before proceeding with the comparisons, we discuss different approaches to error evaluation.

3A. ***Error of the model.*** The natural error norm for elasticity is the energy norm

$$\|\boldsymbol{u}\|_E^2 = \int_\Omega \sigma_{ij}(\boldsymbol{u})\epsilon_{ij}(\boldsymbol{u})\, d\Omega. \tag{3-1}$$

The thin-plate energy norm is

$$\|\boldsymbol{w}\|_S^2 = \int_A (n_{\alpha\beta} w_{\alpha,\beta} - m_{\alpha\beta} w_{3,\alpha\beta})\, dA, \tag{3-2}$$

where w_i is the structural deflection.

The elasticity norm (3-1) is inappropriate for measuring the errors of the plate model considered, due to the constitutive assumption, (2-4). A tight bound on the error in stress for Kirchhoff theory is available

[Simmonds 1971]. However, for the purpose of validating the reduction procedure proposed for the loads, we use a simpler error measure, namely, the *relative error in the energy*

$$\frac{\left(\|\boldsymbol{u}\|_E^2 - \|\boldsymbol{w}\|_S^2\right)^{1/2}}{\|\boldsymbol{u}\|_E}. \tag{3-3}$$

In the case of isotropic torsionless axisymmetric elasticity, the elastic strain energy norm (3-1) is expressed in terms of the radial and transverse displacements (u_r and u_z, respectively) as follows:

$$\|\boldsymbol{u}\|_E^2 = \pi \int_{-t/2}^{t/2}\int_0^a \frac{E}{(1+\nu)}\left\{\frac{2\nu}{(1-2\nu)}\left(u_{r,r}+\frac{u_r}{r}+u_{z,z}\right)^2 + 2\left[(u_{r,r})^2+\left(\frac{u_r}{r}\right)^2+(u_{z,z})^2\right]+(u_{r,z}+u_{z,r})^2\right\} r\,dr\,dz. \tag{3-4}$$

The energy norm for the circular thin-plate $\|\boldsymbol{w}\|_S$ is the sum of a membrane part associated with the in-plane forces and of a bending part associated with the transverse forces

$$\|\boldsymbol{w}\|_S^2 = \underbrace{2\pi\int_0^a \frac{Et}{1-\nu^2}\left[(w_{r,r})^2+\left(\frac{w_r}{r}\right)^2+2\nu\frac{w_{r,r}w_r}{r}\right] r\,dr}_{\text{in-plane}} + \underbrace{2\pi\int_0^a D\left[\left(w_{z,rr}+\frac{1}{r}w_{z,r}\right)^2-2(1-\nu)\frac{w_{z,r}w_{z,rr}}{r}\right] r\,dr}_{\text{transverse}}. \tag{3-5}$$

3B. ***Simply supported circular thin plate under uniform normal load.***

3B.1. *Elasticity solution.* Consider a solid of revolution which is free of body forces and is loaded axisymmetrically by uniform normal tractions $h_z = q$ applied at the surface $z = -t/2$, $0 < r < a$ as shown in Figure 2a. The essential and natural boundary conditions corresponding to simple support on the lateral boundary $r = a$, $-t/2 < z < t/2$ are as follows:

$$g_z = -\frac{qt}{160E}\left\{80(1+2\nu+\nu^2)\frac{z^4}{t^4}+\left[120\nu(1-\nu)\frac{a^2}{t^2}-24(5+2\nu+\nu^2)\right]\frac{z^2}{t^2} + 80\frac{z}{t}-10\nu(1-\nu)\frac{a^2}{t^2}+9+2\nu+\nu^2\right\}, \tag{3-6}$$

$$h_n = -q\,(2+\nu)\,\frac{z}{t}\left(\frac{3}{20}-\frac{z^2}{t^2}\right).$$

In addition, axial symmetry conditions are enforced at the center $r = 0$, $-t/2 < z < t/2$:

$$g_n = 0, \qquad h_z = 0. \tag{3-7}$$

Note that in all examples considered hereafter the prescribed body force and boundary loads are consistent with the desired analytical solution obtained by the semi-inverse method.

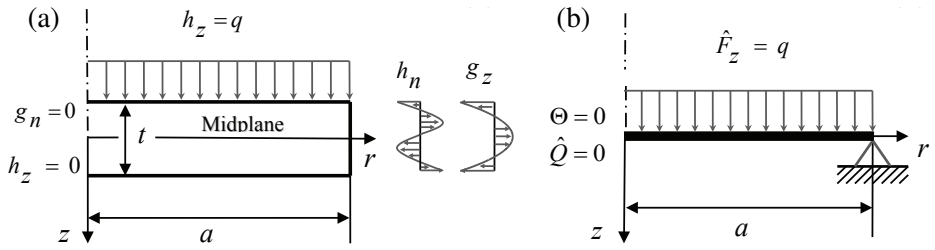

Figure 2. (a) Torsionless axisymmetric thin flat elastic solid under uniform normal tractions. (b) Simply supported circular thin plate under effective uniform transverse force.

The analytical solution, in terms of stress, of the torsionless axisymmetric elasticity problem obtained using Love's stress function is

$$\begin{aligned}
\sigma_{rr} &= q\frac{z}{t}\left[\frac{3\,(3+\nu)}{4}\frac{a^2}{t^2}\left(1-\frac{r^2}{a^2}\right)+(2+\nu)\left(\frac{z^2}{t^2}-\frac{3}{20}\right)\right],\\
\sigma_{\theta\theta} &= q\frac{z}{t}\left\{\frac{3\,(3+\nu)}{4}\frac{a^2}{t^2}\left[1-\frac{(1+\nu)\,r^2}{(3+\nu)\,a^2}\right]+(2+\nu)\left(\frac{z^2}{t^2}-\frac{3}{20}\right)\right\},\\
\sigma_{zz} &= \frac{q}{2}\left(-4\frac{z^3}{t^3}+3\frac{z}{t}-1\right), \qquad \sigma_{rz} = \frac{3q}{4}\frac{r}{t}\left(4\frac{z^2}{t^2}-1\right).
\end{aligned} \tag{3-8}$$

3B.2. *Thin-plate solution.* Using the definitions in Table 1 (with x_3 replaced by z) we obtain the axisymmetric thin-plate load resultants and boundary conditions (thin-plate data) derived from the boundary loads and displacements of the original three-dimensional problem:

$$\begin{aligned}
\hat{F}_z = F_z = q \qquad & (0<r<a),\\
W_z = 0, \qquad M_n = 0 \qquad & (r=a),\\
\Theta = 0, \qquad \hat{Q} = 0 \qquad & (r=0).
\end{aligned} \tag{3-9}$$

Equation (3-9) suggests that the problem corresponds to a thin plate which is simple supported at $r = a$ as shown in Figure 2b. The normal tractions h_3 on the surface $z = -t/2$, $0 < r < a$ of the elastic body contribute to the effective applied transverse force $\hat{F}_z$.

The in-plane reduced problem has a trivial solution. Solving the transverse reduced problem with the data (3-9), we obtain the transverse deflection of the plate

$$w_z = \frac{3qa^4\left(1-\nu^2\right)}{16Et^3}\left(1-\frac{r^2}{a^2}\right)\left(\frac{5+\nu}{1+\nu}-\frac{r^2}{a^2}\right). \tag{3-10}$$

The approximate displacement field $\boldsymbol{u}^s$ is obtained from $\boldsymbol{w}$ using the kinematic assumptions (2-2) and (2-3). Full displacement fields are given in the Appendix. The components of the corresponding thin-plate stress field are as follows — compare (3-8):

$$\sigma^s_{rr} = q\frac{z}{t}\,\frac{3\,(3+\nu)}{4}\frac{a^2}{t^2}\left(1-\frac{r^2}{a^2}\right) \quad \text{and} \quad \sigma^s_{\theta\theta} = q\frac{z}{t}\,\frac{3\,(3+\nu)}{4}\frac{a^2}{t^2}\left[1-\frac{(1+\nu)}{(3+\nu)}\,\frac{r^2}{a^2}\right]. \tag{3-11}$$

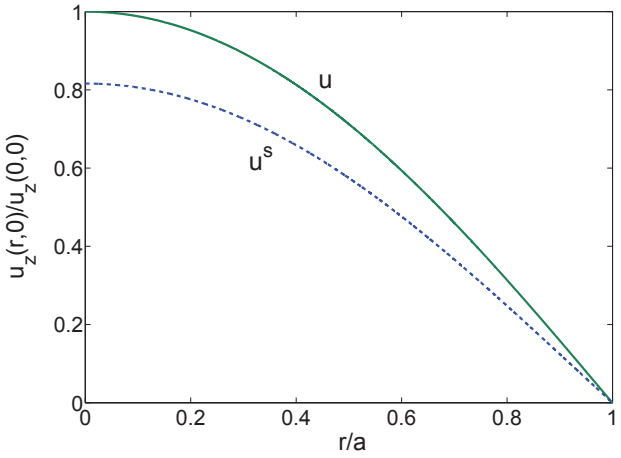

Figure 3. Simply supported circular plate ($t/a = 0.5$, $\nu = 0.3$) under uniform normal load: transverse displacements, $z = 0$.

3B.3. *Error evaluation.*

Relative error of displacement. Figure 3 represents the normalized midplane transverse displacements $u_z/u_z(0,0)$ (solid line) and $u_z^s/u_z(0,0)$ (dashed line) for $t/a = 0.5$ and Poisson's ratio $\nu = 0.3$. Even for this relatively large thickness the error in the structural displacement is relatively small. Recalling that $0 \le z \le t$, $(z/a) \le (t/a)$ and $0 \le r \le a$ one observes that the relative error of the transverse displacement for the circular thin plate in this case tends to zero as $t/a \to 0$ (see also (3-8) and (3-11) for stresses σ_{rr} and $\sigma_{\theta\theta}$ where the first term in the parentheses is dominant for $a/t \gg 1$).

Relative error in energy. The Taylor series expansion of relative error in the energy with respect to the relative thickness t/a up to order five yields

$$\frac{\left(\|\boldsymbol{u}\|_E^2 - \|\boldsymbol{w}\|_S^2\right)^{1/2}}{\|\boldsymbol{u}\|_E} = \frac{2}{5}\sqrt{\frac{30}{(7+\nu)}}\,\frac{t}{a} + \frac{1652 + 2596\nu + 15\nu^2 - 6\nu^3 - \nu^4}{2100\,(1-\nu)\,(7+\nu)}\sqrt{\frac{30}{(7+\nu)}}\,\frac{t^3}{a^3} + \mathcal{O}\left(\frac{t^5}{a^5}\right). \quad (3\text{-}12)$$

One observes that the expression of the relative error in the energy for the simply supported circular thin plate under uniform normal load, (3-12), tends to zero as the ratio of the thickness to the radius of the plate tends to zero (Figure 4).

3C. ***Simply supported circular thin plate under linearly varying tangential load.*** We now consider a different elasticity problem that reduces to the same thin-plate problem as in Section 3B.

3C.1. *Elasticity solution.* A solid of revolution is loaded now by linearly varying tangential tractions $h_r = \pm\frac{q}{2t}r$ (where q is a constant) applied at the surfaces $z = \pm t/2$, $0 < r < a$, as shown in Figure 5a. The essential and natural boundary conditions corresponding to simple support on the lateral boundary

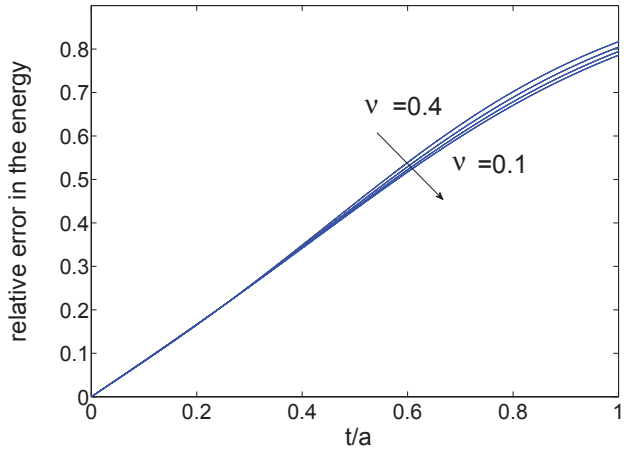

Figure 4. Simply supported circular plate under uniform normal load: relative error in the energy.

$(r = a,\ -t/2 < z < t/2)$ are

$$g_z = -\frac{qt}{160E}\left\{80(1+2\nu+\nu^2)\frac{z^4}{t^4} + \left[120\nu(1-\nu)\frac{a^2}{t^2} - 8(5+6\nu+3\nu^2)\right]\frac{z^2}{t^2} - 10\nu(1-\nu)\frac{a^2}{t^2} + \frac{7}{3} + 2\nu + \nu^2\right\}, \quad (3\text{-}13)$$

$$h_n = -q\,(2+\nu)\,\frac{z}{t}\left(\frac{3}{20} - \frac{z^2}{t^2}\right),$$

while the axial symmetry conditions are satisfied at $r = 0,\ -t/2 < z < t/2$:

$$g_n = 0, \qquad h_z = 0. \quad (3\text{-}14)$$

Note that while here h_n is identical to that given in (3-6), g_z is different.

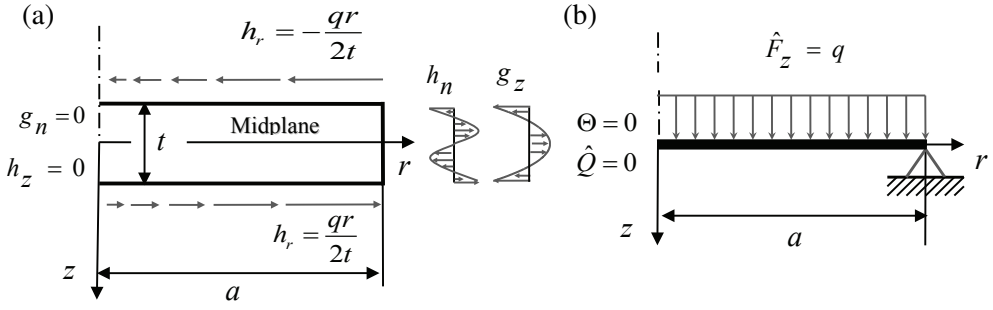

Figure 5. (a) Torsionless axisymmetric thin flat elastic solid under linearly varying tangential tractions. (b) Simply supported circular thin plate under effective uniform transverse force.

The solution of the elasticity problem is as follows:

$$\sigma_{rr} = q\frac{z}{t}\left[\frac{3\,(3+\nu)}{4}\frac{a^2}{t^2}\left(1-\frac{r^2}{a^2}\right)+(2+\nu)\left(\frac{z^2}{t^2}-\frac{3}{20}\right)\right],$$
$$\sigma_{\theta\theta} = q\frac{z}{t}\left\{\frac{3\,(3+\nu)}{4}\frac{a^2}{t^2}\left[1-\frac{(1+\nu)}{(3+\nu)}\frac{r^2}{a^2}\right]+(2+\nu)\left(\frac{z^2}{t^2}-\frac{3}{20}\right)\right\},$$
$$\sigma_{zz} = \frac{q}{2}\left(-4\frac{z^3}{t^3}+\frac{z}{t}\right), \qquad \sigma_{rz} = \frac{3q}{4}\frac{r}{t}\left(4\frac{z^2}{t^2}-\frac{1}{3}\right). \tag{3-15}$$

3C.2. *Thin-plate solution.* The thin-plate data are

$$\hat{F}_z = \frac{1}{r}\frac{\partial}{\partial r}(r\,C_r) = q \qquad (0<r<a), \tag{3-16}$$
$$W_z = 0, \qquad M_n = 0 \qquad (r=a),$$
$$\Theta = 0, \qquad \hat{Q} = 0 \qquad (r=0).$$

The definitions of F_z, W_z, Θ, M_n and $\hat{Q}$ are given in Table 1 (with x_3 replaced by z). Equation (3-16) suggests that the problem corresponds to a thin plate simply supported at $r=a$, as shown in Figure 5b. Only the applied couple C_r that originates in the tractions h_r on the top and bottom surfaces of the elastic body contribute to the effective applied transverse force $\hat{F}_z$.

One observes that the linearly varying tangential tractions are reduced to the same load resultants as for the circular thin plate under uniform normal load derived in Section 3B.2. Thus the transverse deflection of the simply supported circular thin plate is identical to that given by (3-10). The thin-plate stress field is given in (3-11).

3C.3. *Error evaluation.*

Relative error of displacement. Figure 6 represents the normalized midplane transverse displacements

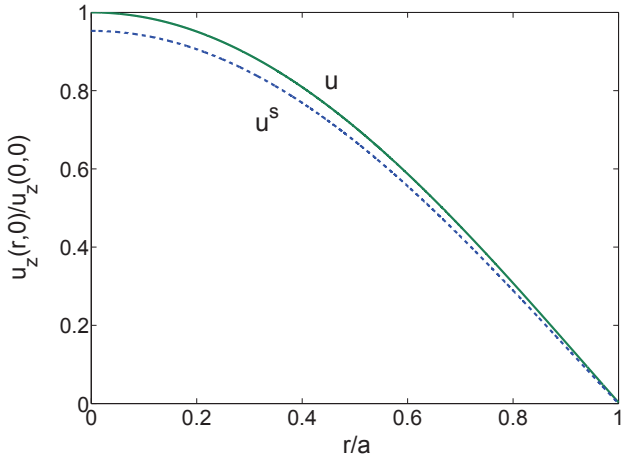

Figure 6. Simply supported circular plate ($t/a = 0.5$, $\nu = 0.3$) under linearly varying tangential load: transverse displacements at $z = 0$.

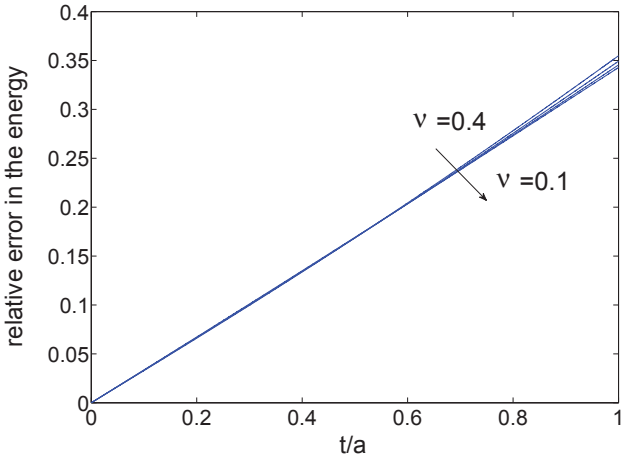

Figure 7. Simply supported circular plate under linearly varying tangential load: relative error in the energy.

$u_z/u_z(0,0)$ (solid line) and $u_z^s/u_z(0,0)$ (dashed line) for $t/a = 0.5$ and Poisson's ratio $\nu = 0.3$. Full displacement fields are given in the Appendix. Once again one observes that the relative error of the transverse displacement for the circular thin plate in this case tends to zero as $t/a \to 0$ (see also (3-15) and (3-11) for stresses).

Relative error in energy. The Taylor series expansion of relative error in the energy with respect to the relative thickness t/a up to order five yields

$$\frac{\left(\|\boldsymbol{u}\|_E^2 - \|\boldsymbol{w}\|_S^2\right)^{1/2}}{\|\boldsymbol{u}\|_E} = \frac{2}{5}\sqrt{\frac{5}{(7+\nu)}}\,\frac{t}{a} + \frac{56+368\nu+45\nu^2-18\nu^3-3\nu^4}{1050\,(1-\nu)\,(7+\nu)}\sqrt{\frac{5}{(7+\nu)}}\,\frac{t^3}{a^3} + \mathcal{O}\left(\frac{t^5}{a^5}\right). \quad (3\text{-}17)$$

We can see that the expression of the relative error in the energy for the simply supported circular thin plate under linearly varying tangential load, (3-17), tends to zero as the ratio of the thickness to the radius of the plate tends to zero (Figure 7). Although the structural reduced problem is identical to the one considered in Section 3B.2, both the relative error in displacements and the relative error in energy are consistently smaller in the case of a plate loaded by a linearly varying tangential tractions (Figures 6 and 7). The reason is the difference in the data of the underlying three-dimensional elasticity problems.

3D. ***Central point supported circular thin plate under linearly varying tangential load.*** We now consider an elasticity problem with the same linearly varying tangential tractions on the top and bottom surfaces of the plate as in Section 3C but different boundary conditions at the center and on the lateral boundary, giving rise to an effective boundary shear force of the thin-plate problem.

3D.1. *Elasticity solution.* The loading applied at the top and bottom surfaces is identical to that considered in Section 3C.1, as shown in Figure 8a. The natural boundary conditions on the lateral boundary

$(r = a,\ -t/2 < z < t/2)$ are

$$h_n = -q\,(2+\nu)\,\frac{z}{t}\left(\frac{3}{20} - \frac{z^2}{t^2}\right), \qquad h_z = \frac{qa}{4t}\left(12\frac{z^2}{t^2} - 1\right). \tag{3-18}$$

The essential boundary conditions at the center $(r = 0,\ -t/2 < z < t/2)$ are

$$g_n = 0,$$
$$g_z = \frac{qt}{160E}\Big\{-80(1+2\nu+\nu^2)\frac{z^4}{t^4} + \Big[-120\nu(3+\nu)\frac{a^2}{t^2} + \big(120+144\nu+72\nu^2\big)\Big]\frac{z^2}{t^2} + 10\nu(3+\nu)\frac{a^2}{t^2} - \frac{7}{3} - 2\nu - \nu^2\Big\}. \tag{3-19}$$

The stress distribution for this elasticity problem is the same as that of the previous problem, (3-15).

3D.2. *Thin-plate solution.* Considering the thin-plate data

$$\begin{aligned} &\hat{F}_z = \frac{1}{r}\frac{\partial}{\partial r}(r\,C_r) = q && && (0 < r < a), \\ &W_z = 0, && \Theta = 0 && (r = 0), \\ &\hat{Q} = -C_r^- = -\tfrac{1}{2}qa, && M_n = 0 && (r = a), \end{aligned} \tag{3-20}$$

one observes that the transverse load $\hat{F}_z$ is identical to the one considered in Section 3C.2 whereas an effective shear force $\hat{Q}$ is applied now at the boundary $r = a$. Equation (3-20) suggests that the problem corresponds to a thin plate which is free at $r = a$ and fixed (central point supported) at $r = 0$, as shown in Figure 8b. Only the applied couple C_r that originates in the tractions h_r on the top and bottom surfaces of the elastic body contributes to the effective applied transverse force $\hat{F}_z$ and effective prescribed boundary shear force $\hat{Q}$ on the edge of the plate.

The transverse deflection of the central point supported circular thin plate is

$$w_z = -\frac{3qa^4\left(1-\nu^2\right)}{16Et^3}\frac{r^2}{a^2}\left(2\,\frac{3+\nu}{1+\nu} - \frac{r^2}{a^2}\right). \tag{3-21}$$

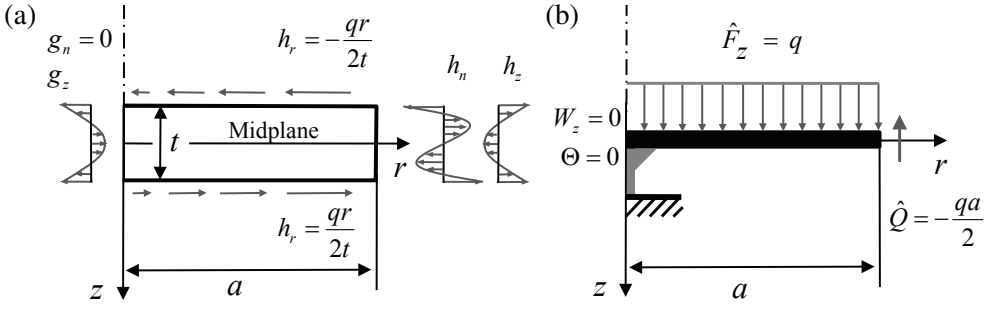

Figure 8. (a) Center-supported torsionless axisymmetric plate-like elastic solid under linearly varying tangential tractions. (b) Central point supported circular thin plate under effective uniform transverse and boundary shear forces.

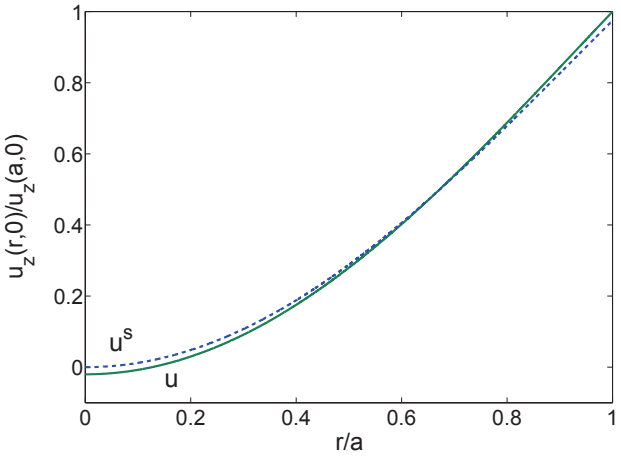

Figure 9. Central point supported circular plate ($t/a = 0.5$, $\nu = 0.3$) under linearly varying tangential load: transverse displacements at $z = 0$.

The approximate three-dimensional structural displacement field $\boldsymbol{u}^s$ is obtained from the kinematic assumptions (2-2) and (2-3). Full displacement fields are given in the Appendix. Note that the thin-plate stress field for the last load case is identical for both previous ones and is given in (3-11). The reason is that the problem considered here is self-equilibrated and the resultant of the distributed transverse load $\hat{F}$ is equal to the resultant of the effective shear force $\hat{Q}$ applied at the boundary $r = a$. As a result, the reaction at the center $r = 0$ of the plate is zero (see Figure 5b) making the stress field of two problems to be identical.

3D.3. *Error evaluation.*

Relative error of displacement. Figure 9 represents the normalized midplane transverse displacements $u_z/u_z(a, 0)$ (solid line) and $u_z^s/u_z(a, 0)$ (dashed line) for $t/a = 0.5$ and Poisson's ratio $\nu = 0.3$. In accordance with Figure 9, the midplane displacement at the center of the plate-like solid (solid line) is not zero whereas the thin plate deflection (the structural problem solution, dashed line) is zero at this point. The reason is in the definition of the structural deflections as displacements averaged through the thickness of the plate-like body rather than the displacements of the midplane (see remark on page 772). The difference between the two solutions corresponds to the rigid body translation and rotation of the plate and does not affect the stress field.

Relative error in energy. Since constants in the relative error in energy corresponding to an axial rigid-body translation may be discarded, the relative error in energy of the central point supported plate is identical to that of the simple supported plate considered in Section 3C.3.

4. Numerical efficiency

Finite element computations illustrate the implementation, as well as the accuracy and efficiency, of the plate formulation proposed for general loading configurations. A comparison of the problem size required to attain a certain level of accuracy by solid elements and thin-plate elements subject to the resultant loads proposed demonstrates the efficiency of the structural model. The load configuration

that is considered would pose a formidable challenge to many conventional approaches to plate loading. Trilinear hexahedral elements with incompatible modes [Taylor et al. 1976] are used for the elasticity solution. Bicubic Hermite Bogner–Fox–Schmit rectangular elements [Bogner et al. 1966; Zienkiewicz and Taylor 2000] are used for the thin-plate problem. This element is restricted to rectangular shapes, limiting the numerical tests to rectangular geometries. It bears emphasis that our structural procedures are subject to no such restriction.

Consider an $a \times a$ plate of aspect ratio $t/a = 0.025$ centered at the origin, undergoing constant rotation ω around the normal axis (Figure 10). The isotropic elastic material has a Poisson ratio $\nu = 0.3$. The density varies linearly through the thickness

$$\rho = \rho_0 \left(1 + \frac{x_3}{2t}\right). \tag{4-1}$$

The three-dimensional loading due to the rotation is represented by an applied body force in the radial direction of magnitude $\rho\omega^2 r$. The transverse structural loading in this problem results solely from distributed couples that arise from the variation of the radial body force. In order to focus on the bending response, we consider only the variable part of the distribution:

$$f_\alpha = \frac{\rho_0 \omega^2}{2t}\, x_\alpha x_3. \tag{4-2}$$

The resultant structural loads are applied couples, computed from the definition in Table 1:

$$C_\alpha = \frac{\rho_0 \omega^2 t^2}{24}\, x_\alpha. \tag{4-3}$$

Clearly, thin-plate formulations that don't account for applied couples are incapable of representing this type of load configuration.

By symmetry, only one quarter of the body is considered in the computation (see Figure 10). We impose free boundary conditions on the outer edges $x_1 = a/2$ and $x_2 = a/2$, and symmetry boundary conditions on the edges $x_1 = 0$ and $x_2 = 0$, and fix the axis of rotation. For the plate problem, consistent nodal loads are computed from the applied couples C_α as indicated by the principle of virtual work (2-11).

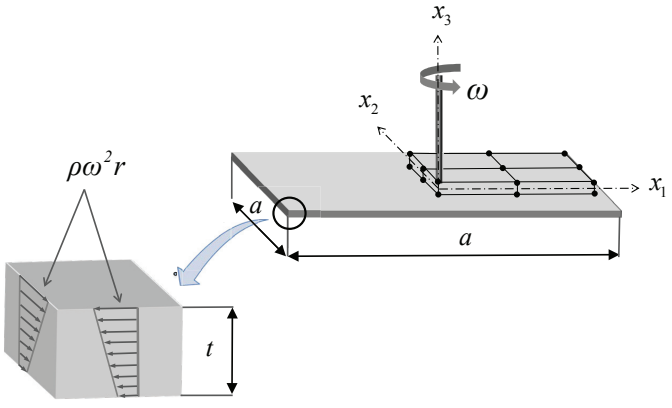

Figure 10. Rotating square plate with varying density: problem statement, the depicted solid mesh is $2 \times 2 \times 1$ (due to symmetry, only one quarter is discretized).

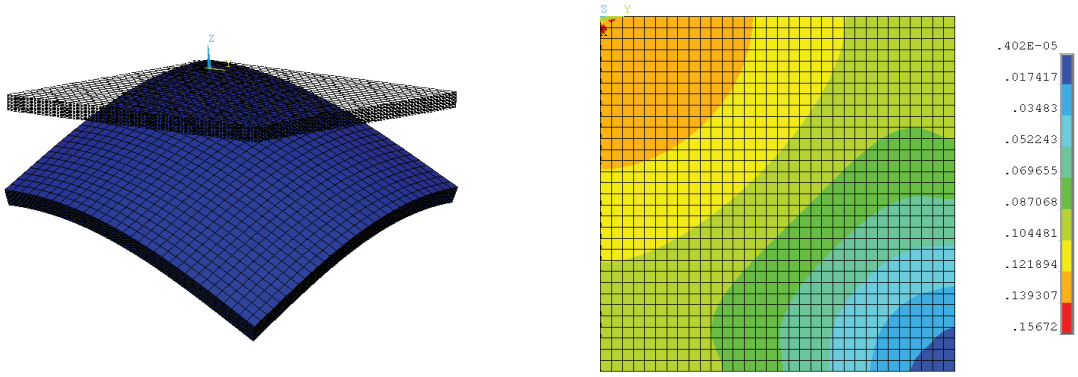

Figure 11. Rotating square plate with varying density: Deformed shape and von Mises stress distribution; 32 × 32 × 16 solid mesh.

Thus, no effective boundary shear force or corner forces are required. Accounting for applied couples is essential for the thin-plate modeling of this problem. Figure 11 shows representative results for the 32 × 32 × 16 solid mesh.

Remark. The applied couples appear explicitly in the variational statement of this problem. In contrast, the loading in the strong form would be expressed in terms of an effective distributed transverse force and effective boundary shear force, both emanating from the applied couples, as well as homogeneous corner force boundary conditions.

A comparison of the number of degrees of freedom in the numerical models of the continuum and structural problems required to attain a certain level of accuracy provides an estimate of the computational efficiency of the structural representation. Let $\boldsymbol{u}^h$ and $\boldsymbol{w}^h$ be the three-dimensional and thin-plate finite element solutions, respectively. The accuracy of both is measured relative to $\boldsymbol{u}^{\text{ref}}$, a converged three-dimensional finite element reference solution obtained on a highly refined mesh (64 × 64 × 32), accounting for the combination of modeling and discretization errors in the thin-plate computations. Since the elastic energy norm (3-1) is inappropriate for measuring errors of the plate models due to the modification of the constitutive law, we use the *relative errors in the energy*

$$\frac{\left(\|\boldsymbol{u}^{\text{ref}}\|_E^2 - \|\boldsymbol{u}^h\|_E^2\right)^{1/2}}{\|\boldsymbol{u}^{\text{ref}}\|_E}, \qquad \frac{\left(\|\boldsymbol{u}^{\text{ref}}\|_E^2 - \|\boldsymbol{w}^h\|_S^2\right)^{1/2}}{\|\boldsymbol{u}^{\text{ref}}\|_E}$$

Results of the comparison are presented in Table 5 and Figure 12. The coarsest plate mesh, 2 × 2 with 24 degrees of freedom, attains a level of accuracy that is comparable with the 16 × 16 × 8 solid model with incompatible modes, that contains 7344 degrees of freedom. The 0.7% error of the converged plate computation is the *modeling error* of the plate theory for this high aspect ratio ($t/a = 0.025$), leading to the high efficiency of the structural representation.

5. Conclusions

The present work describes a systematic conversion of general loads of the classical problem of three-dimensional elastostatics to their thin-plate counterparts. We provide formulas for all types of resultant

	Elasticity					Thin plate			
mesh	2×2×1	4×4×2	8×8×4	16×16×8	32×32×16	2×2	4×4	8×8	16×16
degrees of freedom	36	180	1080	7344	53856	24	80	288	1088
relative error [%]	25.7	14.8	7.6	3.8	1.8	3.2	2.3	0.7	0.7

Table 5. Rotating square plate with varying density: relative error in the energy of the finite element solutions, 3D elasticity with incompatible modes versus thin plate.

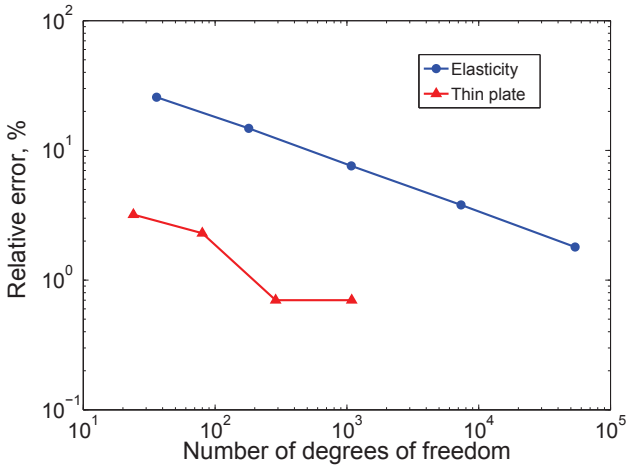

Figure 12. Rotating square plate with varying density: relative error in the energy of the finite element solutions, three-dimensional elasticity with incompatible modes versus thin plate. Reference solution is converged elasticity solution in both cases. The converged plate computation still exhibits a modeling error.

structural loads and boundary conditions in terms of the original three-dimensional data, in forms that are readily incorporated into computational tools, without entailing re-programming of existing software.

The kinematic and constitutive assumptions of Kirchhoff plate theory are substituted into the principle of virtual work for linear elastostatics, leading to a statement of virtual work for the thin plate. This formulation incorporates applied distributed couples engendered by in-plane components of three-dimensional loads, which are rarely accounted for in the context of a thin plate. Disregarding this type of loading may neglect a significant portion of the overall structural response in some cases.

We advocate the treatment of the twisting moment in virtual work in a form that seldom appears in the literature. This simpler form is compatible with the variational statement of higher-order plate theories, and obviates the use of the Kirchhoff equivalent force and corner forces in methods based on virtual work such as finite element analysis, thereby allowing lower regularity of the prescribed boundary twisting moment and facilitating implementation.

Structural essential boundary conditions are imposed on the quantities associated with a variation in the boundary integrals of the Euler–Lagrange equations. The data are specified by a through-the-thickness averaging procedure suggested by the definition of the force resultants. This interpretation of

the structural deflections as through-the-thickness averages of the continuum displacements, rather than their values on the midplane (the more conventional notion), yields explicit formulas for the thin-plate essential boundary data.

In-plane components of three-dimensional body forces and tangential tractions on the top and bottom surfaces engender applied distributed couples, modifying the transverse loading of the plate bending problem. The distributed loading in the equilibrium equation is an effective transverse force. The standard term is modified by the in-plane divergence of the applied couples.

Similarly, the shear loading is an effective boundary shear force. The celebrated Kirchhoff equivalent force is modified by the edge trace of the applied couples. These terms, which are rarely accounted for in the literature, would be difficult to derive intuitively.

When the boundary is not smooth, shear boundary conditions include discrete corner forces defined as jumps of the prescribed boundary twisting moment emanating from tangential tractions applied on the lateral boundary. Corner forces appear in the literature only as reaction forces that are part of the solution in some cases, and in other descriptions there is no mention of corner forces whatsoever. Consistent variational derivation of the plate problem formulation gives rise to the corner forces in the Euler–Lagrange equations, and therefore they should appear explicitly as natural boundary conditions in the problem statement.

Overall, the formulation presented in this work facilitates the solution of problems that would otherwise pose formidable challenges. Numerical results confirm that appropriate use of the thin-plate model economizes computation and provides insight into the mechanical behavior, while preserving a level of accuracy comparable with the full three-dimensional solution.

Appendix: Displacement fields of analytical problems

A. *Simply supported circular thin plate under uniform normal load.*

Elasticity solution.

$$u_r = \frac{qr}{20Et^3}\left\{20(2+\nu-\nu^2)\,z^3+\left[-15(1-\nu^2)\,r^2+15(3-2\nu-\nu^2)\,a^2-(6+27\nu-3\nu^2)\,t^2\right]z+10\nu\,t^3\right\} \tag{A.1}$$

$$\begin{aligned} u_z = \frac{q}{480Et^3}\Big\{&-240(1+2\nu+\nu^2)\,z^4+\left[720\nu(1+\nu)\,r^2-360\nu(3+\nu)\,a^2+(360+144\nu+72\nu^2)\,t^2\right]z^2 \\ &-240\,z\,t^3+90(1-\nu^2)\,r^4-\left[180(3-2\nu-\nu^2)a^2+(288+36\nu+36\nu^2)\,t^2\right]r^2 \\ &+90(5-4\nu-\nu^2)\,a^4+6(48+11\nu+\nu^2)\,a^2\,t^2-(27+6\nu+3\nu^2)\,t^4\Big\} \end{aligned} \tag{A.2}$$

Thin-plate solution.

$$u_r^s = -\frac{3qrz}{4Et^3}\left[(1-\nu^2)\,r^2-(3-2\nu-\nu^2)\,a^2\right] \tag{A.3}$$

$$u_z^s = \frac{3q}{16Et^3}\left[(1-\nu^2)\,r^4-2(3-2\nu-\nu^2)\,r^2\,a^2+(5-4\nu-\nu^2)\,a^4\right] \tag{A.4}$$

B. *Simply supported circular thin plate under linearly varying tangential load.*

Elasticity solution.

$$u_r = \frac{qr}{20Et^3}\left\{20(2+\nu-\nu^2)z^3 + \left[-15(1-\nu^2)r^2 + 15(3-2\nu-\nu^2)a^2 - (6+7\nu-3\nu^2)t^2\right]z\right\} \tag{B.1}$$

$$\begin{aligned} u_z = \frac{q}{480Et^3}\Big\{&-240(1+2\nu+\nu^2)z^4 + \left[720\nu(1+\nu)r^2 - 360\nu(3+\nu)a^2 + (120+144\nu+72\nu^2)t^2\right]z^2 \\ &+ 90(1-\nu^2)r^4 - \left[180(3-2\nu-\nu^2)a^2 + (48+36\nu+36\nu^2)t^2\right]r^2 \\ &+ 90(5-4\nu-\nu^2)a^4 + 6(8+11\nu+\nu^2)a^2t^2 - (7+6\nu+3\nu^2)t^4\Big\} \end{aligned} \tag{B.2}$$

Thin-plate solution. See (A.3) and (A.4).

C. *Central point supported circular thin plate under linearly varying tangential load.*

Elasticity solution.

$$u_r = \frac{qr}{20Et^3}\left\{20(2+\nu-\nu^2)z^3 + \left[-15(1-\nu^2)r^2 + 15(3-2\nu-\nu^2)a^2 - (6+7\nu-3\nu^2)t^2\right]z\right\} \tag{C.1}$$

$$\begin{aligned} u_z = \frac{q}{480Et^3}\Big\{&-240(1+2\nu+\nu^2)z^4 + \left[720\nu(1+\nu)r^2 - 360\nu(\nu+3)a^2 + (120+144\nu+72\nu^2)t^2\right]z^2 \\ &+ 90(1-\nu^2)r^4 - \left[180(3-2\nu-\nu^2)a^2 + (48+36\nu+36\nu^2)t^2\right]r^2 \\ &+ 30\nu(3+\nu)a^2t^2 - (7+6\nu+3\nu^2)t^4\Big\} \end{aligned} \tag{C.2}$$

Thin-plate solution.

$$u_r^s = -\frac{3qrz}{4Et^3}\left[(1-\nu^2)r^2 - (3-2\nu-\nu^2)a^2\right], \quad u_z^s = \frac{3q}{16Et^3}\left[(1-\nu^2)r^4 - 2(3-2\nu-\nu^2)r^2a^2\right] \tag{C.3}$$

References

[Actis et al. 1999] R. L. Actis, B. A. Szabo, and C. Schwab, "Hierarchic models for laminated plates and shells", *Comput. Methods Appl. Mech. Eng.* **172**:1-4 (1999), 79–107.

[Alessandrini et al. 1999] S. M. Alessandrini, D. N. Arnold, R. S. Falk, and A. L. Madureira, "Derivation and justification of plate models by variational methods", pp. 1–20 in *Plates and shells* (Québec, QC, 1996), edited by M. Fortin, CRM Proceedings and Lecture Notes **21**, AMS, Providence, RI, 1999.

[Antman 1995] S. S. Antman, *Nonlinear problems of elasticity*, Applied Mathematical Sciences **107**, Springer, New York, 1995. 2nd ed. published in 2005.

[Bauchau and Craig 2009] O. A. Bauchau and J. I. Craig, *Structural analysis: with applications to aerospace structures*, Solid Mechanics and its Applications **163**, Springer, Dordrecht, 2009.

[Bisegna and Sacco 1997] P. Bisegna and E. Sacco, "A layer-wise laminate theory rationally deduced from the three-dimensional elasticity", *J. Appl. Mech.* (*ASME*) **64**:3 (1997), 538–545.

[Bogner et al. 1966] F. K. Bogner, R. L. Fox, and L. A. Schmit, "The generation of interelement-compatible stiffness and mass matrices by the use of interpolation formulae", pp. 397–443 in *Matrix methods in structural mechanics*, edited by J. S. Przemieniecki et al., Air Force Flight Dynamics Laboratory, Wright-Patterson Air Force Base, OH, 1966. Technical report AFFDL-TR-66-80.

[Calcote 1969] L. R. Calcote, *The analysis of laminated composite structures*, Van Nostrand Reinhold, New York, 1969.

[Ciarlet 1990] P. G. Ciarlet, *Plates and junctions in elastic multi-structures: an asymptotic analysis*, Recherches en Mathématiques Appliquées **14**, Masson, Paris, 1990.

[Ciarlet 1997] P. G. Ciarlet, *Mathematical elasticity, II: Theory of plates*, Studies in Mathematics and its Applications **27**, North-Holland, Amsterdam, 1997.

[Cowper 1966] G. R. Cowper, "The shear coefficient in Timoshenko's beam theory", *J. Appl. Mech.* (*ASME*) **33** (1966), 335–340.

[Dauge and Gruais 1996] M. Dauge and I. Gruais, "Asymptotics of arbitrary order for a thin elastic clamped plate, I: Optimal error estimates", *Asymptot. Anal.* **13**:2 (1996), 167–197.

[Dauge and Gruais 1998] M. Dauge and I. Gruais, "Asymptotics of arbitrary order for a thin elastic clamped plate, II: Analysis of the boundary layer terms", *Asymptot. Anal.* **16**:2 (1998), 99–124.

[DiCarlo et al. 2001] A. DiCarlo, P. Podio-Guidugli, and W. O. Williams, "Shells with thickness distension", *Int. J. Solids Struct.* **38**:6–7 (2001), 1201–1225.

[Engel et al. 2002] G. Engel, K. Garikipati, T. J. R. Hughes, M. G. Larson, L. Mazzei, and R. L. Taylor, "Continuous/discontinuous finite element approximations of fourth-order elliptic problems in structural and continuum mechanics with applications to thin beams and plates, and strain gradient elasticity", *Comput. Methods Appl. Mech. Eng.* **191**:34 (2002), 3669–3750.

[Forte and Vianello 1988] S. Forte and M. Vianello, "On surface stresses and edge forces", *Rend. Accad. Naz. Lincei* **8** (1988), 409–426.

[Grossi and Lebedev 2001] R. O. Grossi and L. Lebedev, "Static and dynamic analyses of anisotropic plates with corner points", *J. Sound Vib.* **243**:5 (2001), 947–958.

[Hu 1984] H.-C. Hu, "Derivation of the classical plate bending theory from elasticity by variational method", *Comput. Struct.* **19**:1–2 (1984), 71–73.

[Hughes 2000] T. J. R. Hughes, *The finite element method: linear static and dynamic finite element analysis*, Dover, Mineola, NY, 2000.

[Hughes and Hinton 1986] T. J. R. Hughes and E. Hinton (editors), *Finite element methods for plate and shell structures*, Pineridge, Swansea, 1986.

[Kirchhoff 1850] G. Kirchhoff, "Über das Gleichgewicht und die Bewegung einer elastischen Scheibe", *J. Reine Angew. Math.* **1850**:40 (1850), 51–88.

[Krylov et al. 2006] S. Krylov, I. Harari, and D. Gadasi, "Consistent loading in structural reduction procedures for beam models", *Int. J. Multiscale Comput. Eng.* **4**:5–6 (2006), 559–584.

[Libai and Simmonds 1998] A. Libai and J. G. Simmonds, *The nonlinear theory of elastic shells*, 2nd ed., Cambridge University Press, Cambridge, 1998.

[Liu and Chang 2005] M.-F. Liu and T.-P. Chang, "Vibration analysis of a magneto-elastic beam with general boundary conditions subjected to axial load and external force", *J. Sound Vib.* **288**:1–2 (2005), 399–411.

[Madureira 2004] A. L. Madureira, "An improved biharmonic model: incorporating higher-order responses of the plate bending phenomena", *Anal. Appl.* **2**:1 (2004), 87–99.

[Moon and Holmes 1979] F. C. Moon and P. J. Holmes, "A magnetoelastic strange attractor", *J. Sound Vib.* **65**:2 (1979), 275–296.

[Morand and Ohayon 1995] H. J.-P. Morand and R. Ohayon, *Fluid structure interaction: applied numerical methods*, Wiley, Chichester, 1995.

[Nádai 1925] A. Nádai, *Die elastischen Platten*, Springer, Berlin, 1925.

[Nayfeh and Pai 2004] A. H. Nayfeh and P. F. Pai, *Linear and nonlinear structural mechanics*, Wiley, Hoboken, NJ, 2004.

[Niordson 1985] F. I. Niordson, *Shell theory*, North-Holland Series in Applied Mathematics and Mechanics **29**, North-Holland, Amsterdam, 1985.

[O'Leary and Harari 1985] J. R. O'Leary and I. Harari, "Finite element analysis of stiffened plates", *Comput. Struct.* **21**:5 (1985), 973–985.

[Podio-Guidugli 2000] P. Podio-Guidugli, "Recent results in the theory of elastic plates", *Transport Theory Stat. Phys.* **29**:1-2 (2000), 217–224.

[Poisson 1829] S. D. Poisson, "Mémoire sur l'équilibre et le mouvement des corps élastiques", *Mém. Acad. Sci. Paris* **8** (1829), 357–570.

[Prescott 1942] J. Prescott, "Elastic waves and vibrations of thin rods", *Philos. Mag. Ser. 7* **33**:225 (1942), 703–754.

[Reismann 1988] H. Reismann, *Elastic plates: theory and application*, Wiley, New York, 1988.

[Reissner 1969] E. Reissner, "On generalized two-dimensional plate theory, II", *Int. J. Solids Struct.* **5**:6 (1969), 629–637.

[Rubin 2000] M. B. Rubin, *Cosserat theories: shells, rods and points*, Solid Mechanics and its Applications **79**, Kluwer Academic, Dordrecht, 2000.

[Sayir and Mitropoulos 1980] M. Sayir and C. Mitropoulos, "On elementary theories of linear elastic beams, plates and shells", *Z. Angew. Math. Phys.* **31**:1 (1980), 1–55.

[Simmonds 1971] J. G. Simmonds, "An improved estimate for the error in the classical, linear theory of plate bending", *Q. Appl. Math.* **29** (1971), 439–447.

[Soedel 1981] W. Soedel, *Vibrations of shells and plates*, Mechanical Engineering **10**, Marcel Dekker, New York, 1981.

[Sokolnikoff 1983] I. S. Sokolnikoff, *Mathematical theory of elasticity*, 2nd ed., Krieger, Malabar, FL, 1983.

[Sutyrin and Hodges 1996] V. G. Sutyrin and D. H. Hodges, "On asymptotically correct linear laminated plate theory", *Int. J. Solids Struct.* **33**:25 (1996), 3649–3671.

[Szilard 2004] R. Szilard, *Theories and applications of plate analysis: classical, numerical and engineering methods*, Wiley, Hoboken, NJ, 2004.

[Taylor et al. 1976] R. L. Taylor, P. J. Beresford, and E. L. Wilson, "A non-conforming element for stress analysis", *Int. J. Numer. Methods Eng.* **10**:6 (1976), 1211–1219.

[Timoshenko 1983] S. P. Timoshenko, *History of strength of materials*, Dover, New York, 1983.

[Timoshenko and Goodier 1951] S. P. Timoshenko and J. N. Goodier, *Theory of elasticity*, 2nd ed., McGraw-Hill, New York, 1951.

[Timoshenko and Woinowsky-Krieger 1959] S. P. Timoshenko and S. Woinowsky-Krieger, *Theory of plates and shells*, 2nd ed., McGraw-Hill, New York, 1959.

[Todhunter and Pearson 1960] I. Todhunter and K. Pearson, *A history of the theory of elasticity and of the strength of materials, vol. I, II*, Dover, New York, 1960.

[Tsiatas 2009] G. C. Tsiatas, "A new Kirchhoff plate model based on a modified couple stress theory", *Int. J. Solids Struct.* **46**:13 (2009), 2757–2764.

[Ugural 1981] A. C. Ugural, *Stresses in plates and shells*, McGraw-Hill, New York, 1981.

[Vasil'ev and Lur'e 1992] V. V. Vasil'ev and S. A. Lur'e, "On refined theories of beams, plates, and shells", *J. Compos. Mater.* **26**:4 (1992), 546–557.

[Vidoli and Batra 2000] S. Vidoli and R. C. Batra, "Derivation of plate and rod equations for a piezoelectric body from a mixed three-dimensional variational principle", *J. Elasticity* **59**:1–3 (2000), 23–50.

[Vogelius and Babuška 1981] M. Vogelius and I. Babuška, "On a dimensional reduction method, I: The optimal selection of basis functions", *Math. Comput.* **37**:155 (1981), 31–46.

[Šolín 2006] P. Šolín, *Partial differential equations and the finite element method*, Wiley, Hoboken, NJ, 2006.

[Wells and Nguyen 2007] G. N. Wells and T. D. Nguyen, "A C^0 discontinuous Galerkin formulation for Kirchhoff plates", *Comput. Methods Appl. Mech. Eng.* **196**:35–36 (2007), 3370–3380.

[Zienkiewicz and Taylor 2000] O. C. Zienkiewicz and R. L. Taylor, *The finite element method, II: Solid mechanics*, 5th ed., Butterworth-Heinemann, Oxford, 2000.

Received 13 Jul 2010. Revised 28 Dec 2010. Accepted 7 Jan 2011.

ISAAC HARARI: harari@eng.tau.ac.il
School of Mechanical Engineering, Tel Aviv University, Ramat-Aviv, 69978 Tel Aviv, Israel
http://www.eng.tau.ac.il/~harari

IGOR SOKOLOV: sokoliv@gmail.com
School of Mechanical Engineering, Tel Aviv University, Ramat-Aviv, 69978 Tel Aviv, Israel

SLAVA KRYLOV: vadis@eng.tau.ac.il
School of Mechanical Engineering, Tel Aviv University, Ramat-Aviv, 69978 Tel Aviv, Israel

JOURNAL OF MECHANICS OF MATERIALS AND STRUCTURES

jomms.org

Founded by Charles R. Steele and Marie-Louise Steele

See http://jomms.org for submission guidelines.

JoMMS (ISSN 1559-3959) is published in 10 issues a year. The subscription price for 2011 is US $520/year for the electronic version, and $690/year (+$60 shipping outside the US) for print and electronic. Subscriptions, requests for back issues, and changes of address should be sent to Mathematical Sciences Publishers, Department of Mathematics, University of California, Berkeley, CA 94720–3840.

JoMMS peer-review and production is managed by EditFLOW™ from Mathematical Sciences Publishers.

PUBLISHED BY
mathematical sciences publishers
http://msp.org/

A NON-PROFIT CORPORATION

Typeset in LaTeX

Journal of Mechanics of Materials and Structures

Volume 6, No. 5 May 2011

Study of multiply-layered cylinders made of functionally graded materials using the transfer matrix method Y. Z. Chen 641

Computational shell mechanics by helicoidal modeling, I: Theory Teodoro Merlini and Marco Morandini 659

Computational shell mechanics by helicoidal modeling, II: Shell element Teodoro Merlini and Marco Morandini 693

Effective property estimates for heterogeneous materials with cocontinuous phases Patrick Franciosi, Renald Brenner and Abderrahim El Omri 729

Consistent loading for thin plates Isaac Harari, Igor Sokolov and Slava Krylov 765

1559-3959(2011)6:5;1-B